Leveraging the benefits of GaN to improve motor system efficiency and power density in robotics applications

Design and experimental evaluation of an ultra-low profile GaN-based motor drive

By
Martin Wattenberg, Staff System Application Engineer for GaN-based systems, Infineon Technologies

Introduction

Robotics is an interdisciplinary field with a strong focus on integration and system optimization. Applications include service robots, collaborative as well as industrial robots, autonomous drones, and automated guided vehicles.

An optimized design of the motors and drives in these robotic applications is key for a successful end-product. In a conventional, silicon-based (Si) design, there is always a trade-off between size and efficiency. For example, smaller size for components such as filters or DC link capacitance can be achieved with higher switching frequency at the cost of increased switching loss.

However, with the recent introduction of gallium-nitride (GaN) high electron mobility transistors (HEMT) in the landscape of power electronics, new design possibilities have been emerging, and the long-standing trade-off between efficiency vs. size seems to be possible to overcome.

Architecture and design solutions for GaN-based motor drives

Figure 1 introduces a top-level schematic of Infineon's 100 V GaN-based motor drive. The primary building block for this motor drive is an optimized half-bridge circuit, with two 100 V, 3 mΩ CoolGaN™ HEMTs in 3x5 mm^2 PQFN lead-frame packages[1] each, having an exposed die on the top side for dual-sided cooling. The half-bridge was designed with minimal power loop inductance in mind. The total loop inductance of 400 pH allows the CoolGaN™ HEMT 100 V to switch on and off in approximately 1 ns without exceeding its peak drain voltage rating. Further improvements have been achieved by minimizing the mutual coupling of the gate and drain current thanks to orthogonal current flow and minimized common source inductance.

[1] samples are already available; contact support@infineon.com

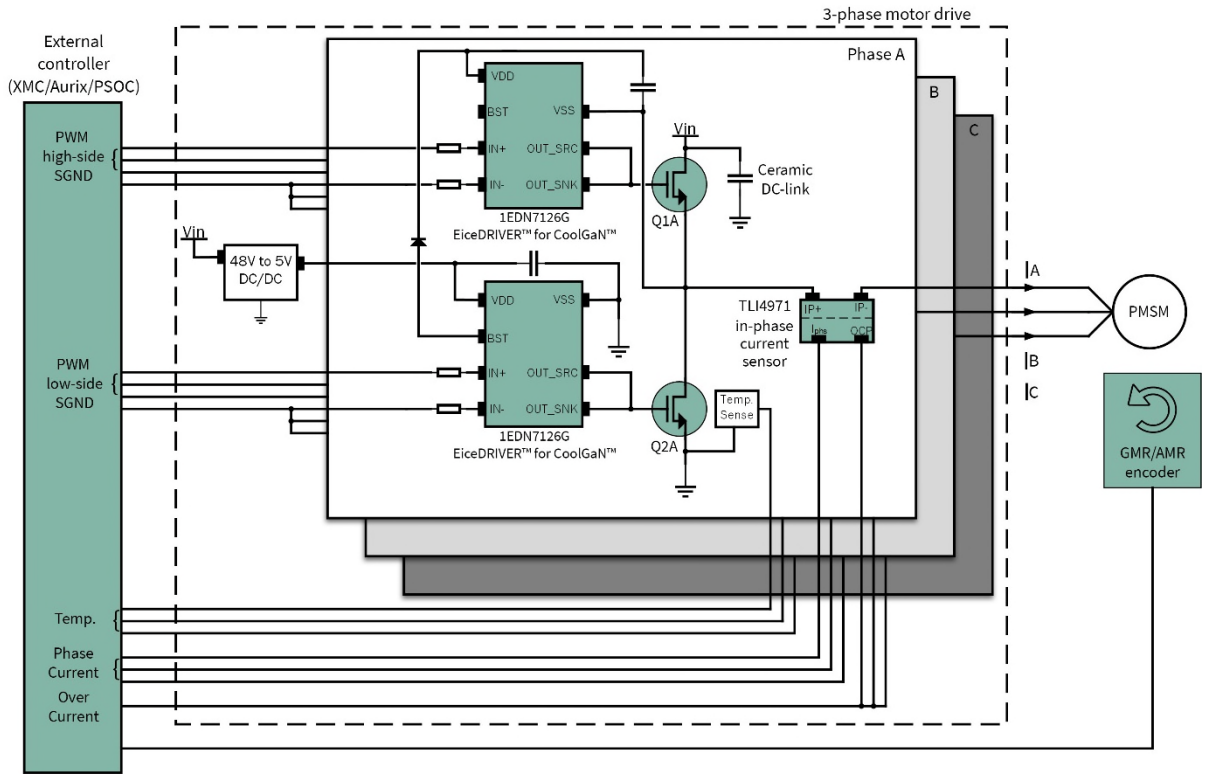

Figure 1. *Schematic of the CoolGaN™ 100 V-based motor drive*

The recommended gate driver is the 1EDN71x6G[2] EiceDRIVER™ for CoolGaN™, which incorporates several key features intended and important to GaN gate driving. The 1EDN7126G was selected in the design on Figure 1, offering 1.5 A peak source/sink current.

One feature of the 1EDN71x6G EiceDRIVER™ for CoolGaN™ products family is the “truly differential input” (TDI), which provides common-mode voltage rejection to the high-side during switching, as well as ground-bounce immunity for the low-side, thereby guaranteeing stable operation even during fast switching transients. Secondly, the driver is available in four different driving strengths so that the turn-on and -off speeds can be adjusted without the need for external gate resistors. Finally, the selected 1EDN7126G gate driver provides an active Miller clamp in the output stage, which amplifies the pull-down strength to 5 A within 3 ns after the gate voltage has fallen below 0.4 V. After the driver latches in this state, it holds the gate voltage at 0 V with a very strong pull-down resistance of 0.3 Ω. In this way, the designer can adjust the GaN HEMT’s turn-off speed without jeopardizing its immunity to induced turn-on.

Each of the three half-bridges includes individual temperature and in-phase current sensing. The total DC link capacitance is over 80 µF, using low-profile 100 V ceramics distributed throughout both sides of the board. The high switching frequency reduces the ripple current burden on these capacitors, avoiding the need for bulkier electrolytic capacitors.

The system also includes a 48 V to 5 V DC/DC converter, which provides a regulated supply voltage to the low-side gate drivers. The high-side gate driver is supplied through bootstrapping, using the active bootstrap clamping feature of the 1EDN71x6G EiceDRIVER™.

[2] This product family will be available soon.

In-phase current sensing was chosen instead of low-side shunt current sensing to fully optimize the high-frequency power loop inductance of the half-bridge and minimize the common-source inductance in the gate loops. The XENSIV™ TLI4971 Hall effect sensor avoids potential common-mode transient immunity (CMTI) issues with differential amplifiers. A well-isolated in-phase current sensor is more immune to voltage transients and provides accurate readings for field-oriented control of the motor.

The control was implemented using an XMC4400 drive card, using sensorless field-oriented control (FOC) firmware with a maximum switching frequency of 100 kHz and a control loop update rate of 20 kHz. Increasing the control frequency to match the switching frequency at 100 kHz would enable even higher control bandwidth for applications that benefit from an extremely fast dynamic control response. Furthermore, in applications where a sensored FOC scheme is preferred, Infineon's XENSIV™ TLE5012 magnetic angle sensors with 0.01° resolution can be used for precise positioning.

Figure 2 shows the top, side, and bottom views of the GaN-based motor drive prototype. The circle with 64 mm diameter, drawn on the front silkscreen, indicates the tightest area encompassing all components needed for a complete motor drive system in a round form factor. This area includes the transistors, drivers, current and temperature sensors, 5 V and 3.3 V regulators, mounting holes for optional heat spreaders, and all capacitors in the system. The dimensions are even smaller in a rectangular form factor: 56 mm x 40 mm, with a total thickness of 3.7 mm, resulting in a total volume of 8.3 cm^3. Considering the targeted power-handling capability of 1 kW, the power density for this motor drive is 120 W/cm^3 or 2 kW/in^3. For laboratory evaluation, the PCB size was slightly increased to include standoffs, high-current screw terminals, and an interface connector to the external control board. Although this evaluation was performed with an external control board, it is evident in Figure 2 that a controller circuit could be added to the bottom side of the PCB without enlarging the total PCB area.

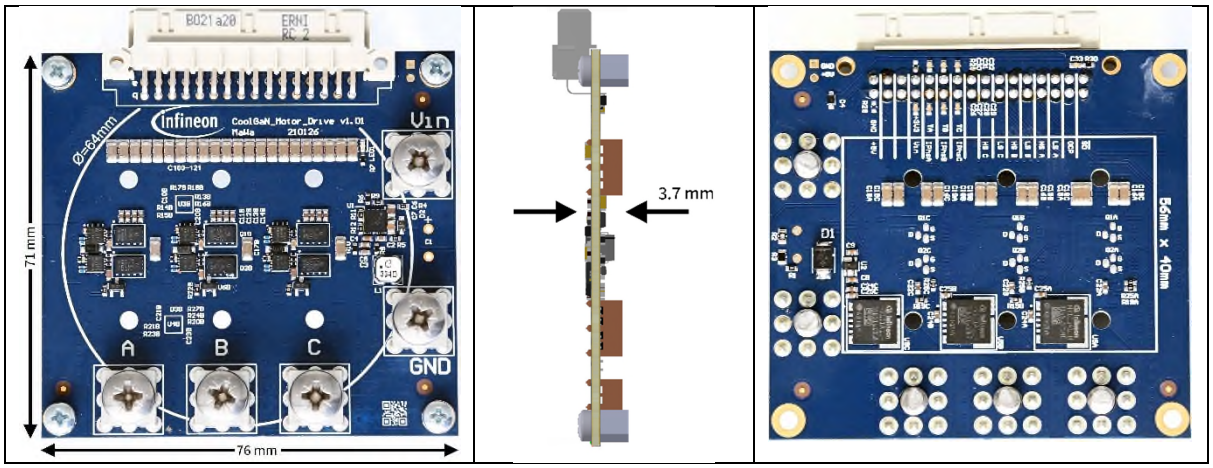

Figure 2. *Top, profile, and side view of CoolGaN™ motor drive.* **Note**: *the entire motor drive, including DC link, current sensors, and auxiliary power supply, can be implemented in a rectangular area of 56 mm x 40 mm.*

It is common to limit the switching speed in motor drives based on a rule-of-thumb such as 5 V/ns. Two potential limiting factors on motor dV/dt are the breakdown of winding insulation and the degradation in the bearings. The winding insulation is not as much of a concern for 48 V motors, where the insulation is typically rated for a much higher voltage. Bearing degradation may still be a concern for some 48 V motor technologies. However, more in-depth research shows that the

severity of this effect depends on many factors, such as motor size and speed, switching frequency, dV/dt, and temperature [1,2]. In addition, the cables connecting the drive to the motor have a significant impact on the dV/dt experienced by the motor.

Impact of motor cables on switching transitions

This article investigates the different slew rates of the phase-to-phase voltage V_{AB} measured in different system positions, from the PCB switch node to the motor. The dV/dt across the device is an important metric for system efficiency and thermal limitation, as longer hard turn-on transitions result in higher switching losses. Using CoolGaN™ 100 V, turn-on transitions as fast as 1 ns can be achieved, leading to minimal switching loss. Figure 3 shows the voltage transient for a hard turn-on and hard turn-off at 16 A, respectively. The hard turn-on transitions in Figure 3 shows a high transition speed of about 50 V/ns, measured differentially across phase A and B. However, when the same measurement is repeated at the end of the 40 cm motor cable, the transition speed is significantly reduced. With a braided cable the, dV/dt is reduced to 8 V/ns. With conventional parallel cables, this is even further reduced to 5 V/ns. If the cable inductance does not provide adequate decoupling of the motor from the high dV/dt at the switch node, a small air coil can be introduced to enable this decoupling effect without additional filter components [3].

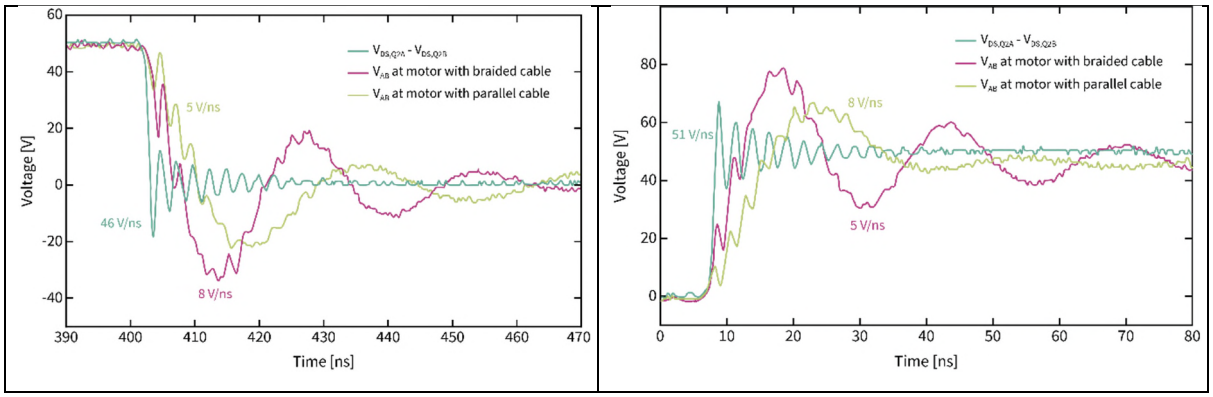

Figure 3. *Hard turn-on and turn-off of low side on the left and right, respectively. In both cases switching current was at 16 A.*

Increased system efficiency due to higher switching frequency

The fast switching speed of CoolGaN™ devices gives power electronics designers the freedom to liberally choose a higher switching frequency, looking at the end-to-end efficiency and total size of the design rather than only at the inverter efficiency.

To highlight the impact of switching frequency on end-to-end system efficiency, an agricultural drone motor was controlled by the CoolGaN™-based motor drive with 20, 60, and 100 kHz switching frequency. The electrical DC input power to the inverter and the mechanical output power of the motor were measured by multimeter and dynamometer, respectively. Figure 4 shows the phase current waveform for 100 W and 500 W operation at 20 and 100 kHz for comparison. The higher switching frequency provides a significantly reduced current ripple leading to lower RMS current, thus less heating of the winding and higher motor efficiency. For operation at 100 W, the RMS current is reduced by 20 percent, from 5.6 to 4.5 A, and for 500 W operation, it is reduced by 12 percent, from 26.2 to 23.1 A.

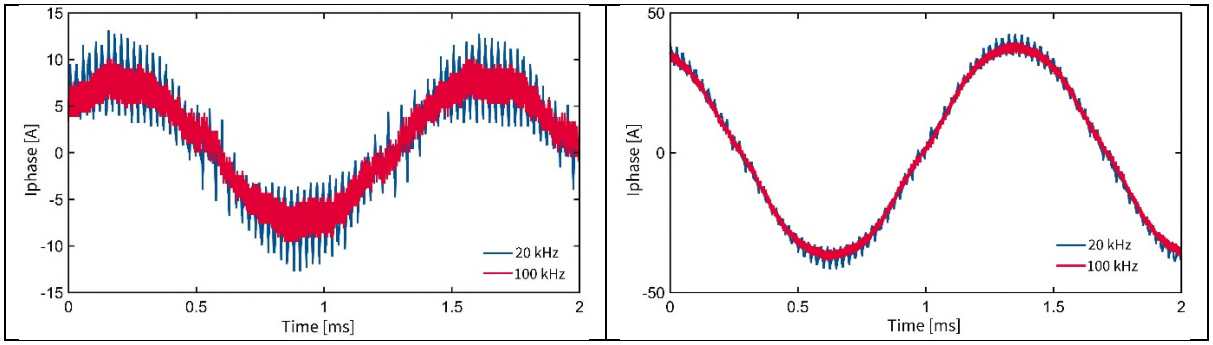

Figure 4. *Phase current waveforms compared at 20 and 100 kHz for 100 W (left) and 500 W (right) operation.*

Even though the benefit of higher switching frequency is more apparent at light load when looking at the relative reduction of RMS phase current, the benefits are very noticeable when looking at the winding temperature over the load range. At 500 W mechanical output power, the winding temperature drops by 30°C from 110°C at 20 kHz to about 80°C at 100 kHz switching frequency (Figure 5). In thermally constrained applications like cobots, this provides a significant advantage.

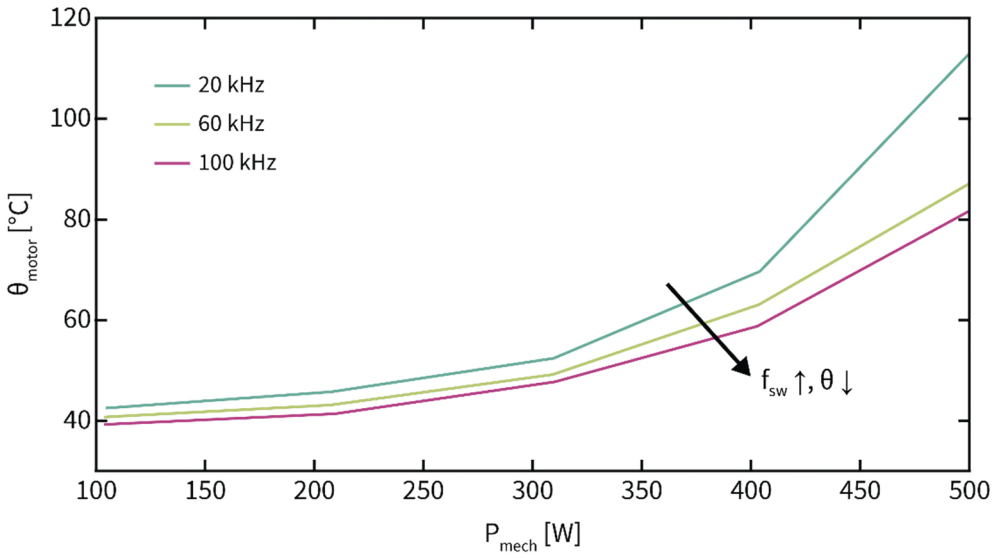

Figure 5. *Motor winding temperature for 20, 60, and 100 kHz operation. Higher switching frequency reduces loss and, therefore, the temperature in the motor.*

The lower current ripple in the motor reduces winding and core loss while lowering the motor temperature. On the other hand, switching loss scales linearly with the switching frequency, thereby increasing the power loss and temperature of the HEMTs. For a Si MOSFET or IGBT, this trade-off would be unfavorable to the system.

However, Figure 6 shows that the end-to-end efficiency, defined by the mechanical output power divided by the electrical input power, can be improved with a higher switching frequency.

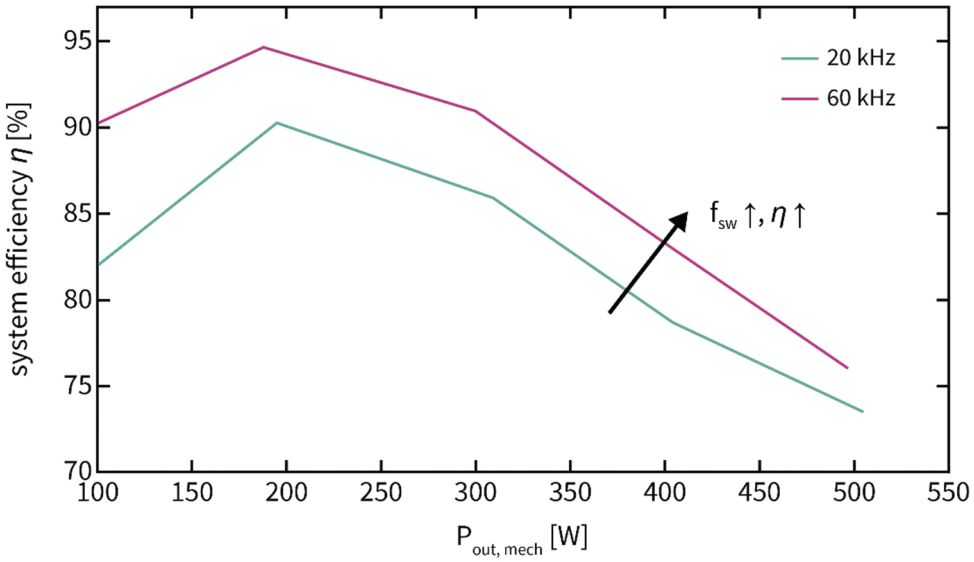

Figure 6. *End-to-end efficiency for 20 and 60 kHz. Higher switching frequency provides an overall improvement to system efficiency.*

Summary

This article presented Infineon's design of a GaN-based motor drive for 48 V applications using a sensorless FOC scheme. It has been developed using CoolGaN™ HEMTs (100 V, 3 mΩ), EiceDRIVER™ gate drivers optimized for CoolGaN™ (1EDN7126G), in-phase XENSIV™ current sensors (TLI4971), and external control from the XMC4400 drive card.

The experimental evaluation of this design clearly showed that GaN enables a higher switching frequency without any measurable penalty to system efficiency or thermal limits. The higher frequency results in lower motor temperature and higher end-to-end system efficiency while also improving power density by reducing the bulk capacitance requirement. Due to the smaller system size, the motor drive can be embedded at the motor chassis, e.g., inside a robot arm, eliminating EMI problems stemming from the long motor cables.

Additionally, measurements of voltage slew rates at several points in the system have shown that the switching speed of the GaN HEMTs can be optimized independently of the applied voltage slew rate at the motor windings, owing to the inherent LC filter effect of the motor cable.

For more information on Infineon's motor drive solutions for robotics, please visit our web.

References

[1] A. Muetze, "Bearing currents in inverter-fed AC motors," Ph.D. dissertation, Dept. Elektrotechnik und Informationstechnik, Technische Universität Darmstadt, DE, 2004.

[2] Y. Xu, et al., "Experimental Assessment of High-Frequency Bearing Currents in an Induction Motor Driven by a SiC Inverter," in IEEE Access, vol. 9, pp. 40540-40549, 2021

[3] Zheyu Zhang, “Decoupling of Interaction Between WBG Converter and Motor Load for Switching Performance Improvement” in Proc. IEEE Applied Power Electronics Conference and Exposition, Long Beach, CA, USA, 2016.